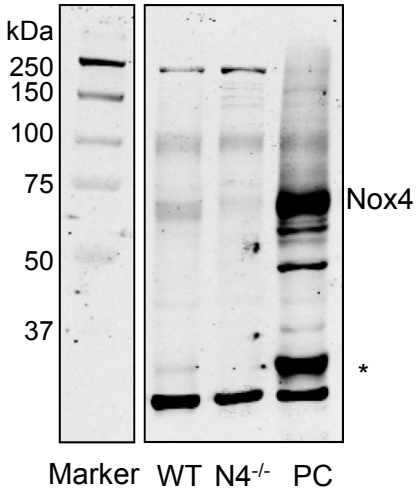

Supplemental Figure 1: Western Blot of Nox4 in bones using an antibody kindly provided by A.M. Shah (King's college, London) showing Nox4 and a degradation product of Nox4 (*). For additional information about specificity of Nox4 detection see Babelova et al. FRBM 2012. WT: wild type mice; N4-/-: Nox4 knockout mice; PC: positive control (WT kidney lysate)

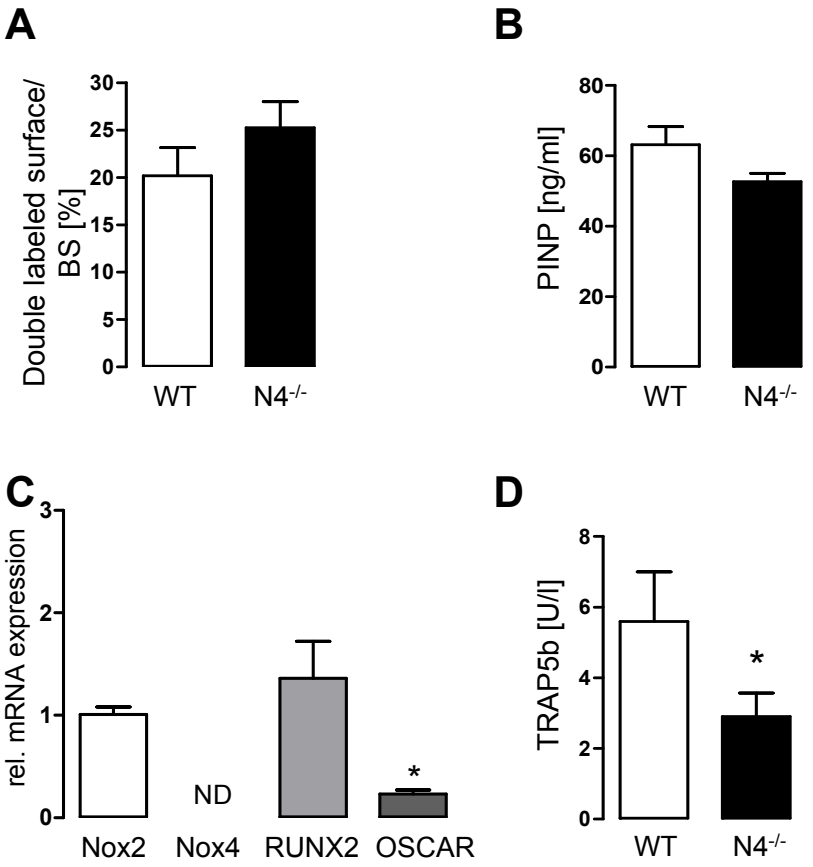

Supplemental Figure 2: (A) Bone formation expressed as double labeled surface as determined by bone histomorphometry in bones of WT and Nox4$^{-/-}$ mice. (B) Serum levels of bone formation marker P1NP. (C) mRNA expression of Nox2, Nox4, RUNX2 and OSCAR in bones from Nox4-/- mice relative to wild type mice. (D) Serum levels of bone resorption marker TRAP5b in WT and Nox4$^{-/-}$ mice. WT: wild type mice; N4-/-: Nox4 knockout mice; n=5-8; *p<0.05; data are mean ± SEM

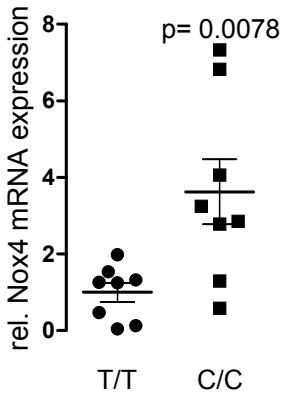

Supplemental Figure 3: Nox4 mRNA expression in human B Lymphocytes with (C/C) and without (A/A) the SNP rs11018628 differentiated with vitamin D3 (10 ng/ml) for 3 days . n=8; data are mean ± SEM

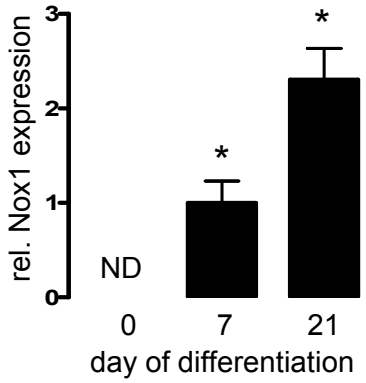

Supplemental Figure 4: mRNA expression of Nox1 in the course of differentiation of human precursor cells into osteoclasts. (day 0, Nox1 was not detectable). ND: not detectable; n=5; *p<0.05; data are mean ± SEM

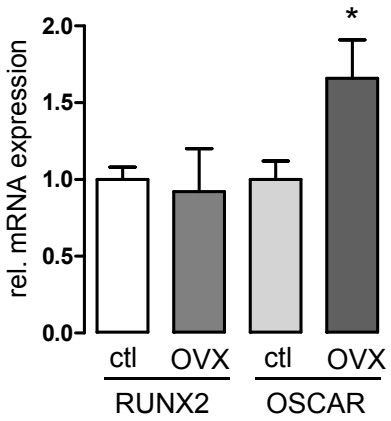

Supplemental Figure 5: mRNA expression of RUNX2 and OSCAR in bones of healthy and ovariectomized mice. n=5-8; *p<0.05; data are mean ± SEM